NeuroImage: Clinical 4 (2014) 517–525

Contents lists available at ScienceDirect

NeuroImage: Clinical

journal homepage: www.elsevier.com/locate/ynicl

Impact of neonate haematocrit variability on the longitudinal relaxation time of blood: Implications for arterial spin labelling MRI

J.B. De Vis[a,*], J. Hendrikse[a], F. Groenendaal[b], L.S. de Vries[b], K.J. Kersbergen[b], M.J.N.L. Benders[b], E.T. Petersen[a,c]

[a] Department of Radiology, University Medical Center Utrecht, Utrecht, The Netherlands
[b] Department of Neonatology, University Medical Center Utrecht, Utrecht, The Netherlands
[c] Department of Radiotherapy, University Medical Center Utrecht, Utrecht, The Netherlands

ARTICLE INFO

Article history:
Received 21 November 2013
Received in revised form 13 March 2014
Accepted 14 March 2014

Keywords:
Blood T_1
Neonates
Arterial spin labelling
Cerebral blood flow
Haematocrit
MRI

ABSTRACT

Background and purpose: The longitudinal relaxation time of blood (T_{1b}) is influenced by haematocrit (Hct) which is known to vary in neonates. The purpose of this study was threefold: to obtain T_{1b} values in neonates, to investigate how the T_{1b} influences quantitative arterial spin labelling (ASL), and to evaluate if known relationships between T_{1b} and haematocrit (Hct) hold true when Hct is measured by means of a point-of-care device.

Materials and methods: One hundred and four neonates with 120 MR scan sessions (3 T) were included. The T_{1b} was obtained from a T_1 inversion recovery sequence. T_{1b}-induced changes in ASL cerebral blood flow estimates were evaluated. The Hct was obtained by means of a point-of-care device. Linear regression analysis was used to investigate the relation between Hct and MRI-derived R_1 of blood (the inverse of the T_{1b}).

Results: Mean T_{1b} was 1.85 s (sd 0.2 s). The mean T_{1b} in preterm neonates was 1.77 s, 1.89 s in preterm neonates scanned at term-equivalent age (TEA) and 1.81 s in diseased neonates. The T_{1b} in the TEA was significantly different from the T_{1b} in the preterm ($p < 0.05$). The change in perfusion induced by the T_{1b} was −11% (sd 9.1%, $p < 0.001$). The relation between arterial-drawn Hct and R_{1b} was $R_{1b} = 0.80 \times \text{Hct} + 0.22$, which falls within the confidence interval of the previously established relationships, whereas capillary-drawn Hct did not correlate with R_{1b}.

Conclusion: We demonstrated a wide variability of the T_{1b} in neonates and the implications it could have in methods relying on the actual T_{1b} as for instance ASL. It was concluded that arterial-drawn Hct values obtained from a point-of-care device can be used to infer the T_{1b} whereas our data did not support the use of capillary-drawn Hct for T_{1b} correction.

1. Introduction

The haematocrit in neonates fluctuates with gestational and postnatal age; with the advance of gestation the mean haematocrit level progressively increases, and in the first 28 days after birth a more or less linear decrease in haematocrit occurs (Jopling et al., 2009). The haematocrit concentration of preterm born neonates declines for an even longer period after birth (8–12 weeks) and has a lower nadir compared to the physiologic anaemia of term newborns (Palis and Segel, 1998). This is caused by a rapid body growth resulting in haemodilution, a shorter lifespan of the red blood cells, poor iron stores and the liver being the primary source of erythropoietin production initially (Salsbury, 2001). In addition, the haematocrit in neonates is known to have a wider variability (28–67%) (Christensen,

Abbreviations: ASL, arterial spin labelling; CBF, cerebral blood flow; $CBF_{1.6}$, cerebral blood flow quantified with a T_{1b} of 1.6 s; $CBF_{1.85}$, cerebral blood flow quantified with a T_{1b} of 1.85 s; CBF_{cor}, cerebral blood flow quantified with the corrected T_{1b}; CBF_{mean}, cerebral blood flow quantified with the mean T_{1b} found in our study; Hct, haematocrit; Hct_{cd}, haematocrit measured on a capillary-drawn blood sample; Hct_{ad}, haematocrit measured on an arterial-drawn blood sample; MRI, magnetic resonance imaging; NPD, normalized perfusion difference; PCA, postconceptional age; PNA, postnatal age; POCT, point-of-care test; R_{1b}, longitudinal relaxation rate constant of blood; T_{1b}, longitudinal relaxation time of blood; TEA, term-equivalent age.

* Corresponding author at: Department of Radiology, University Medical Center Utrecht, HP E 01.132, P.O. Box 85500, 3508 GA Utrecht, The Netherlands.
E-mail address: j.devis-2@umcutrecht.nl (J.B. De Vis).

2213-1582/$ - see front matter
http://dx.doi.org/10.1016/j.nicl.2014.03.006

2000; Geaghan, 2005) compared to the haematocrit in adult subjects (38–46%) (Chanarin, 1984). The spin-lattice or longitudinal relaxation time of blood (T_{1b}) is linearly dependent on haematocrit due to the fast exchange regime of water protons between the blood cell and plasma compartment of blood. In-vitro measurements, performed on bovine blood, confirmed the linear dependency of the venous T_{1b} on haematocrit ($1/T_{1b} = 0.83 \times \mathrm{Hct} + 0.28$), and this within a normal haematocrit range of 0.38–0.46 (Lu et al., 2004). Based on these data and assuming an average haematocrit value of 0.42, the T_{1b} is commonly assumed to be 1.6 s (Gevers et al., 2011; Massaro et al., 2013). However, recent in vivo studies performed in adult subjects found longer T_{1b}; 1.85 s (Qin et al., 2011) and 1.78 s (Shimada et al., 2012), possibly due to higher methaemoglobin levels in 'in vitro' blood samples (Farahani et al., 1999). Similar higher values (1.80 s) were found by Varela et al. (in the neonatal population, although with a wider range (1.40–2.00 s) which is thought to be caused by the larger spread in haematocrit (Varela et al., 2011). In this specific population, a linear relationship between the venous T_{1b} and haematocrit has been demonstrated as well under the form of $1/T_{1b} = 0.50 \times \mathrm{Hct} + 0.37$. The T_{1b} is an important parameter in black-blood angiography (Edelman et al., 1991), the vascular space occupancy technique (Lu et al., 2003) and arterial spin labelling MRI (Williams et al., 1992). Therefore, errors in the T_{1b} estimate may have important implications regarding image quality and accuracy of the methods. An accurate estimate of the T_{1b} may be obtained by T_{1b}-mapping (Qin et al., 2011; Varela et al., 2011; Wu et al., 2010). Because blood T_1 sequences and their postprocessing tools are not readily available on most MR platforms, a good alternative would be to estimate the T_{1b} from haematocrit (Lu et al., 2004; Shimada et al., 2012; Varela et al., 2011). The existing relationships between the T_{1b} and neonatal haematocrit are obtained from experiments in which the haematocrit values were determined with either a spinning or a sedimentation technique (Varela et al., 2011). However, in clinical practice, a point-of-care test (POCT), which deduces haematocrit from for instance conductivity measurements, is commonly used to determine the haematocrit in neonates. This technique is known to introduce errors in haematocrit measurements as its accuracy is dependent on the preanalytical and analytical steps; a delay in testing, total protein and lipid levels, sodium concentration and erythroblasts may influence the haematocrit estimate (Abbott Point of Care Inc., 2013). Neonates are known to have lower protein content compared to adults (Ehrnebo et al., 1971) which may artificially decrease haematocrit estimate (Abbott Point of Care Inc., 2013), total parenteral nutrition can induce hyperlipidaemia (Proytcheva, 2009) which can lead to an overestimation of the haematocrit (Abbott Point of Care Inc., 2013), and one study found an overestimation of the haematocrit count with a POCT which was explained by the interference of erythroblasts (Papa et al., 2011). Therefore, it is sensible to evaluate the relation between POCT-obtained haematocrit and the T_{1b} before estimating the T_{1b} from haematocrit using previous established relations.

The purpose of this study is therefore twofold. First, to evaluate the T_{1b} in neonates, at the same time investigating its impact on quantitative arterial spin labelling perfusion estimates. Second, to evaluate if the established relationships between haematocrit and T_{1b} also hold true for the more commonly available capillary-drawn or arterial-drawn point-of-care estimates of haematocrit.

2. Materials and methods

2.1. Subjects

The ethics committee of our institution approved this retrospective study and waived the requirement to obtain written parental informed consent. Neonates with MR imaging between September 2011 and December 2013 were included. Of the 104 neonates 51 neonates were male and 53 neonates were female. In 16 of the 104 neonates (8 males, 8 females) follow-up MR imaging was performed. Data of all 120 MR scans were used for data analysis. The mean age of the study subjects at the time of MR imaging was 40 weeks postconceptional age (range = 30–54 weeks). In our institution, preterm born infants are imaged at preterm age and at term-equivalent age for research purposes. Therefore, subjects were categorized into the following categories. 1) Preterm: neonates with MR imaging at preterm age. 2) TEA: preterm born neonates with MR imaging at term-equivalent age. 3) Diseased: neonates with a clinical indication for MR imaging. In the latter category, 27 infants were diagnosed with perinatal asphyxia, 14 infants were suspected for stroke or MR imaging was performed for follow-up after stroke, 4 infants were imaged after surgery to evaluate white matter damage, 3 infants were suspected for haemorrhage on ultrasound images or MRI was performed for follow-up after haemorrhage, 2 infants had a viral infection with neurological symptoms, and 1 infant with a developmental venous anomaly and 1 infant with a twin-to-twin transfusion syndrome were imaged. Mean (range) postconceptional age at birth, mean (range) postnatal age at the time of MR imaging, gender and the breathing condition are shown for each category in Table 1.

2.2. Laboratory analysis

Haematocrit (Hct) was measured using a point-of-care device in 66 infants (16 preterms, 13 TEA and 37 diseased) within 24 h of MR imaging, 46 blood samples were capillary-drawn ($\mathrm{Hct_{cd}}$) and 20 arterial-drawn ($\mathrm{Hct_{ad}}$). For this, a test cartridge blood analysis system (Abbott i-STAT System, Abbott Laboratories, Abbott Point of Care Inc., Princeton, New Jersey) was used. This system consists of microfabricated sensors housed in a cartridge which measure the conductivity. The measured conductivity, after correction for electrolyte concentration, is inversely related to the haematocrit. Estimates of imprecision for this device, performed on adult blood and evaluated against other point-of-care tests using either conductivity or optical technology, ranged from 0.46% to 1.31%, and a test–retest study found a coefficient of variation of 1.5% (Abbott Point of Care Inc., 2013). For our measurements, capillary-drawn blood was collected by pricking the skin of the infants' heel and arterial-drawn blood was collected via an umbilical line or through a line in the radial artery. During blood collection, the infants were in supine position.

2.3. Image acquisition

All MRI studies were performed on a 3.0 Tesla Philips Achieva System (Philips Medical Systems, Best, The Netherlands). Images were acquired using the quadrature body coil for transmission. An 8-element phased-array head coil was used as a signal receiver. In neonates imaged at preterm age a 4-element flex coil was used (SENSE Flex L + S) as signal receiver. A neonatologist was present throughout the entire examination. Monitoring of heart rate, respiratory rate (Philips, Best, The Netherlands) and transcutaneous oxygen saturation (Nonin Pulse Oxymetry, Nonin Medical, Plymouth, MN) was performed during MR imaging. In infants with artificial breathing support, the ventilation pressure was set to maintain a stable oxygen saturation of 90–95% in preterm infants and 95–100% in infants imaged at term-equivalent age. Prior to MR imaging neonates were sedated; chloral hydrate was administered orally (50–60 ml/kg), in neonates scanned around 3-months equivalent age an intramuscular injection of pethidine, chlorpromazine and promethazine was used. In order to minimize motion-related artefacts neonates were wrapped into an MR-compatible vacuum cushion. For hearing protection MiniMuffs (Natus Europe, Münich, Germany) and earmuffs (EM's 4 Kids, Everton Park, Australia) were used. In addition to the conventional MR imaging scan protocol a localizer MR angiography slab, a T_1 inversion recovery sequence (Varela et al., 2011) and pulsed ASL perfusion imaging were performed. The T_1 inversion recovery sequence consisted of a single

Table 1
Subject characteristics.

Group	N	PCA_b (weeks)	PNA (days)	Gender	Breathing
Preterm	18	28 (24–34)	25 (7–42)	7 M–11 F	SIMV: 3 infants CPAP: 10 infants BiPAP: 2 infants Independent: 3 infants
TEA	50	28 (24–34)	89 (36–119)	24 M–26 F	Independent: 50 infants
Diseased	52	39 (33–42)	20 (1–103)	28 M–24 F	SIMV: 16 infants CPAP: 3 infants Independent: 33 infants

PCA_b, postconceptional age at birth; PNA, postnatal age when MR imaging was performed; TEA, term-equivalent age; M, male; F, female; SIMV, synchronized intermittent mandatory ventilation; CPAP, continuous positive airway pressure; BiPAP, bilevel positive airway pressure.
PCA_b, mean (range) PNA, the number of male and female infants and their breathing condition at the time of MR imaging for each category of neonates; preterm, TEA: preterm born infants with MR imaging at TEA, diseased: infants with a clinical indication for MR imaging.

adiabatic inversion pulse followed by a single-shot echo-planar imaging as readout (Varela et al., 2011). The adiabatic inversion pulse was preceded by a presaturation pulse (Fig. 1a). Scan parameters were; TR/TE/ΔTI/TI_1: 15 s/20 ms/140 ms/20 ms, 50 phases, scan matrix 128 × 128, FOV 160 × 160, flip angle 95°, slice thickness 3 mm and SENSE 2.5. The imaging plane of the T_1 inversion recovery sequence was positioned perpendicular to the superior sagittal sinus based on the sagittal angiography image. Arterial spin labelling MR imaging consisted of a pulsed star labelling of arterial regions (PULSAR) pulse sequence (Golay et al., 2005) followed by a multi-slice, single-shot echo-planar imaging readout. Scan parameters of the ASL sequence were: matrix 40 × 40, FOV 160 × 128 mm, SENSE 2.5, voxel size 4 × 4 × 7 mm, gap between slices 1 mm, TR/TE: 2700/17 ms, flip angle 90°, inversion delay (TI_2) 1500 ms, 70 averages, labelling slab 10 cm, gap between imaging plane and labelling plane 1 cm, no vascular crushers and scan time 3:20 min. To obtain a finite bolus length a saturation pulse was applied in the labelling region 600 ms (TI_1 = 600 ms) after the labelling pulse using the Q_2TIPS technique (Luh et al., 1999). Eleven slices were acquired in ascending slice order. Planning of the imaging plane was performed based on sagittal T_1-weighted images.

2.4. Image analysis

Images were analysed using IDL 6.1 for Windows (ITT Visual Information Solutions, Boulder, CO, U.S.A.). The T_{1b} was estimated from the T_1 inversion recovery data. First, automatic localization of the sagittal sinus was performed on the magnitude reconstructed data; at later time points, the inflowing blood signal is high (fully recovered) while the surrounding 'static' tissue is suppressed by the repeated acquisition at high flip angle (Fig. 1c). This allows for automatic detection of the sagittal sinus by searching for the largest connected high intensity region in the posterior region. The combination of voxels which resulted in the smallest overall residual error of the fit was subsequently chosen from within the initial region-of-interest (Fig. 1b). This selection was based on the goodness of fit of the individual voxels within the region of interest where the best fits were incrementally averaged until the overall residual errors reached a minimum. These voxels were then averaged and used for the subsequent analysis. The T_{1b} was derived from the inversion recovery curve using a standard two parameter inversion recovery model (Varela et al., 2011):

$$S(t) = M_0\left(1 - 2e^{-\frac{t}{T_1}}\right) \quad (1)$$

where $S(t)$ is the signal over time, M_0 is the magnetization, t is the time and T_1 is the longitudinal relaxation of blood.

Data obtained during ASL imaging were processed as follows. First, ASL images were motion corrected using a two-step approach. A 6 parameter affine transformation between (control-label) image pairs was applied, followed by a 12 parameter affine transformation to get all control-label volume pairs aligned. Subsequently, the ASL imaging pairs were subtracted to generate ΔM images. The mean and standard deviation of the difference signal over the subtracted image pairs were calculated and image pairs with a difference signal larger than 2 standard deviations of the mean were automatically discarded (Oguz et al., 2003). The remaining ΔM images were averaged to create ΔM_{total} images and CBF was quantified (Fig. 1d) using the following formula (Buxton, 2005; Luh et al., 1999):

$$f = \frac{\lambda \Delta M}{2\alpha M_{0t} T I_1 e^{\frac{-TI_2}{T_{1b}}}} \quad (2)$$

with f the cerebral blood flow, λ the brain–blood partition coefficient, ΔM the total magnetization difference between control and label images, α the inversion efficiency, M_{0t} the tissue magnetization, TI_1 the bolus length (600 ms), TI_2 the inversion delay (1500 ms) and T_{1b} the longitudinal relaxation time of blood. The α and the λ were assumed to be 95% and 1.1 ml/g (Herscovitch and Raichle, 1985), respectively, the latter represents an average whole-brain neonatal λ value. The T_{1b} was set at 1.6 s based on a recent ASL study in neonates (Massaro et al., 2013) although most earlier studies use an even shorter T_{1b} of typically 1.5 s (Miranda et al., 2006; Wintermark et al., 2011). Whole brain CBF values were obtained and called ($CBF_{1.6}$). Hereafter, CBF was quantified with the T_{1b} derived from the inversion recovery sequence (CBF_{cor}, corrected CBF) and with the mean T_{1b} found in our study population (CBF_{mean}).

2.5. Data analysis

IBM SPSS Statistics (version 19.0.1, SPSS Inc., Chicago, IL) was used for statistical analysis. For all analyses, a p-value lower than 0.05 was considered statistically significant. For the T_{1b} fitting, a 95% confidence interval of the final fitted T_{1b} was estimated based on a bootstrap resampling of the fitting residuals (Efron, 1979). This confidence interval was expressed as percentage of the individual's mean T_{1b} and the average interval was calculated for the entire group as well as for each category. Mean T_{1b}, standard deviation and range were calculated for all neonates and within each category of neonates. An independent sample t-test was used to compare the T_{1b} in ventilated infants to the T_{1b} in infants who were not ventilated and to compare the T_{1b} between the preterm and the TEA. In the infants with both MR imaging at preterm age and at TEA, a paired sample t-test was used to compare the T_{1b} at preterm to the T_{1b} at TEA. Likewise, a paired sample t-test was used to compare $CBF_{1.6}$ to CBF_{cor} for all infants and for the infants with longitudinal data. The normalized perfusion difference (NPD) was calculated: $NPD = ((CBF_{cor} - CBF_{1.6}) / CBF_{1.6}) \times 100$. A one-sample t-test was used to test the null hypothesis; "the normalized perfusion difference equals zero". Similarly, we calculated the normalized perfusion difference when going from CBF quantified with the mean T_{1b} found in this study (CBF_{mean}) to CBF quantified

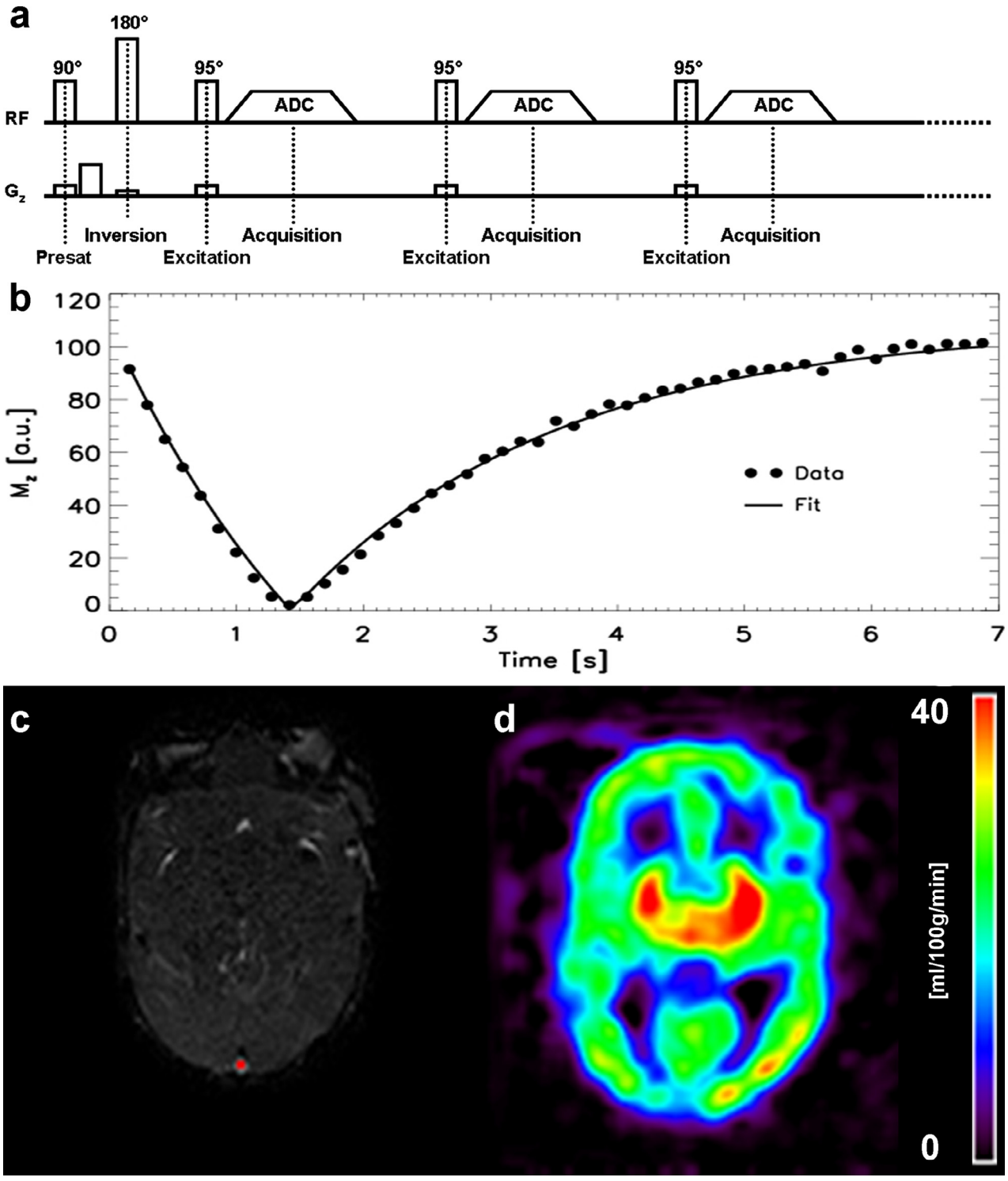

Fig. 1. a) MR sequence chart of the T_1 inversion recovery sequence. The T_1 inversion recovery sequence consisted of a presaturation pulse followed by an adiabatic inversion pulse and a single-shot echo-planar imaging as readout. b–d) Data of a preterm born female infant with MR imaging at term-equivalent age, the postconceptional age of this infant at birth was 26 weeks and MR imaging was performed at 41 weeks. b) Example plot of the acquired data, obtained in the final ROI (which was composed of 5 voxels) within the sagittal sinus, and its corresponding fit. c) Repeated acquisition at a high flip angle ensures saturation of brain tissue and allows for only inflowing blood to be imaged. An automatic localizer tool (red dot) localizes the sagittal sinus based on signal intensity. d) Example of a quantitative arterial spin labelling image.

with the individual-derived T_{1b} (CBF_{cor}); NPD = ((CBF_{cor} − CBF_{mean}) / CBF_{mean}) × 100. An independent sample *t*-test was used to compare the mean normalized perfusion difference (CBF_{cor} versus $CBF_{1.6}$) between preterm and TEA and to investigate if the increase in perfusion from preterm to TEA was significant. In infants with both haematocrit and T_{1b} we investigated the relation between R_{1b} ($1/T_{1b}$) and haematocrit by means of linear regression analysis. The coefficients of determination (R^2) were calculated to evaluate the fit of the models. In those infants, the haematocrit at preterm age was compared to the haematocrit at TEA using an independent sample *t*-test.

2.6. Simulations

As the T_{1b} is known to depend not only on the haematocrit but also on the oxygenation level of blood (Lu et al., 2004; Silvennoinen et al., 2003), errors may occur in the T_{1b}–haematocrit relationship due to not measuring the T_{1b} in fully oxygenated blood. In order to evaluate this error a simulation was performed based on evidence from the existing literature. The dependence of the T_{1b} as a function of haematocrit (Hct) and oxygen saturation (Y) has been shown to have the form (Grgac et al., 2012):

$$T_{1b}(\mathrm{Hct}, \mathrm{Y}) = \frac{1}{(F_{ery,w}(\mathrm{Hct}) \cdot (\mathrm{A} + \mathrm{B} \cdot (1 - \mathrm{Y})) + (1 - F_{ery,w}(\mathrm{Hct})) \cdot \mathrm{C})} \quad (3)$$

where T_{1b}(Hct, Y) is the longitudinal relaxation time of blood as a function of haematocrit and oxygenation and $F_{ery,w}$(Hct) is the fraction of water in the whole blood that resides inside erythrocytes as a function of haematocrit (Eq. (3) in Grgac et al., 2012). Solving this equation with data presented at 3 T (Lu et al., 2004) results in A = 0.97 s^{-1}, B = 0.52 s^{-1} and C = 0.36 s^{-1} which was used to assess the possible error in the T_{1b}–Hct relationship as a result of not measuring the T_{1b} in fully oxygenated blood.

In this paper, the normalized perfusion difference was evaluated based on the effect of haematocrit on the T_{1b} (Lu et al., 2004; Varela et al., 2011). However, λ in Eq. (2) is also known to be haematocrit dependent with an opposite effect than the T_{1b} and therefore also affects the normalized perfusion difference. In order to investigate the overall normalized perfusion difference a simulation was performed. For this, λ–Hct relationships obtained from the literature (Herscovitch and Raichle, 1985) were used together with the established T_{1b}–Hct relationship obtained in this study and results of this were compared against a constant T_{1b} and a constant λ (1.1 ml/g).

3. Results

The T_{1b} could be derived from the inversion recovery curve in 82 out of 120 MR imaging sessions (68%). In these, the mean (standard deviation, sd) number of voxels selected by the automatic localizer was 5 (3). Mean T_{1b} was 1.85 (0.2) s and ranged from 1.4 s to 2.3 s. The average 95% confidence interval of the T_{1b} fitting was [−2.26%, 2.31%]. No significant difference was found in the T_{1b} of ventilated infants (n = 18, T_{1b} is 1.78 (0.19)) versus the T_{1b} of infants who were not ventilated (n = 64, T_{1b} is 1.87 (0.21)). Mean T_{1b} in the preterm was 1.77 (0.14) s, 1.89 (0.19) s in the TEA, and 1.81 (0.24) s in the diseased. These values, the ranges and the 95% confidence interval of the T_{1b} fitting are shown in Table 2. Fig. 2a shows median, interquartile distance, minimum and maximum T_{1b} values for each category in a boxplot. The T_{1b} was significantly different in the preterm than in the TEA ($p < 0.05$). In 6 (out of 8) infants with MR imaging at preterm and at TEA the T_{1b} could be derived from the inversion recovery sequence at both time points. The mean postconceptional age at preterm in these infants was 30 (1) weeks and the mean T_{1b} at preterm age was 1.76 (0.17) s. The mean postconceptional age at TEA in these 6 infants was 41 (1) weeks and the mean T_{1b} was 1.99 (0.13) s. In these 6 infants, the T_{1b} at preterm was significantly different from the T_{1b} at TEA ($p < 0.05$). The mean postnatal age of all the infants was 49 (42) days and ranged from 1 to 119 days. The relation between T_{1b} and postnatal age (PNA, in days) is shown in Fig. 2b. In this figure each colour represents a category of infants.

In 76 of the 82 infants in whom the T_{1b} was derived from the inversion recovery sequence, whole brain CBF was evaluated. For this analysis, an average of 10.5 (3)% of the ASL images was automatically discarded due to motion artefacts. Mean $CBF_{1.6}$ was 17.3 (10.9) ml/100 g/min and CBF_{cor} was 14.5 (10.4) ml/100 g/min. These were significantly different ($p < 0.001$). The mean normalized perfusion difference was −11 (9.1)% and the difference ranged from −27.3% to 13.5% ($p < 0.001$). As the mean T_{1b} found in this study was 1.85 s, we quantified CBF with a T_{1b} of 1.85 s and calculated the normalized perfusion difference when going from $CBF_{1.85}$ (=CBF_{mean}) to CBF_{cor}. The mean normalized perfusion difference was 2 (10.4)% and the difference ranged from −16.8% to 29.9%. For each category of infants (preterms, TEA and diseased) the CBF values ($CBF_{1.6}$, CBF_{cor} and $CBF_{1.85}$) and their corresponding normalized perfusion differences are shown in Table 3, the mean postconceptional age at the time of MRI with ASL whole brain CBF values was 31 (2) weeks for the preterms, 41 (1) weeks for the TEA and 43 (6) weeks for the diseased infants. The normalized perfusion difference, when going from $CBF_{1.6}$ to CBF_{cor}, was significantly different in all preterm than in all the TEA infants ($p < 0.05$). The maturational increase in perfusion was 195% on the $CBF_{1.6}$ images ($p < 0.01$) compared to 178% on the CBF_{cor} images ($p < 0.01$). Of the 6 infants with MRI T_{1b} data at preterm and term-equivalent age whole brain CBF was evaluated at both time points in 4 infants. In these 4 infants, the normalized perfusion difference, when going from $CBF_{1.6}$ to CBF_{cor}, was −4.1 (11.8)% at preterm age and −18.5 (3.8)% at term-equivalent age, this did not reach significance ($p = 0.051$). The maturational increase in perfusion of these 4 infants was 167% on the $CBF_{1.6}$ images compared to 135% on the CBF_{cor} images.

In 39 neonates both haematocrit and T_{1b} were available; in 10 preterms mean haematocrit was 0.4 (0.04), in 12 TEA infants it was 0.34 (0.06) and in 17 diseased infants mean haematocrit was 0.46 (0.07). The haematocrit in the preterms was significantly different from the haematocrit in the TEA ($p < 0.01$). The relation between R_{1b} and haematocrit was investigated and was generally moderate: R_{1b} = 0.38 [0.16–0.61] × Hct + 0.41 [0.31–0.50] (N = 39, R^2 = 0.25, $p < 0.001$), with the 95% confidence interval shown between brackets. The haematocrit data was further subdivided into capillary-drawn (n = 29) and arterial-drawn (n = 10) haematocrit. Capillary-drawn haematocrit was obtained from 9 preterm, 12 TEA and 8 diseased neonates. Arterial-drawn haematocrit was obtained from 1 preterm and 9 diseased neonates. The relation between R_{1b} and arterial-drawn haematocrit was R_{1b} = 0.80 [0.39–1.22]·Hct_{ad} + 0.22 [0.03–0.40] (R^2 = 0.71, $p < 0.01$). This was stronger than the relation between R_{1b} and capillary-drawn haematocrit: R_{1b} = 0.25 [−0.02–0.51]·Hct_{cd} + 0.46 [0.35–0.57] (R^2 = 0.12, p = 0.69). In Fig. 3, the relation between haematocrit and MRI-derived T_{1b} is shown. The relation between R_{1b} and haematocrit was investigated both for ventilated infants and for the infants who were not ventilated. For the ventilated infants (n = 17) the relation was; R_{1b} = 0.41 [−0.35–0.85] × Hct + 0.40 [0.21–0.59], R^2 = 0.21. For the nonventilated infants (n = 22) the relation was R_{1b} = 0.36 [0.07–0.66] × Hct + 0.41 [0.29–0.53], R^2 = 0.25, $p < 0.05$.

A simulation of the dependence of the T_{1b} on haematocrit and oxygenation (Y) is shown in Fig. 4a. In this figure the variation in the T_{1b} for different haematocrit values and oxygenation levels is shown. This figure demonstrates that for a similar haematocrit value T_{1b} is expected to change around 200 ms when going from a low venous oxygenation level of 40% to an arterial oxygenation level of close to 100%. A second simulation (Fig. 4b) demonstrates the normalized perfusion difference introduced by the influence of haematocrit on the T_{1b}, this with and without taking the influence of haematocrit on the brain–blood partition coefficient (λ) into account. From this figure

Table 2
T_1 of blood in categories of neonates.

	T_1 of blood			
	N	Mean (sd) (s)	Range (s)	95% CI (%)
Preterm	11	1.77 (0.14)	1.42–1.90	−3.21, 3.13
TEA	43	1.89 (0.19)	1.51–2.30	−2.14, 2.28
Diseased	28	1.81 (0.24)	1.46–2.35	−2.06, 2.03

This table shows the mean (standard deviation, sd), the range and the 95% confidence interval (95% CI) of the T_{1b} within each category of infants; preterm, TEA: preterm born infants with MR imaging at term-equivalent age, diseased: infants with a clinical indication for MR imaging.

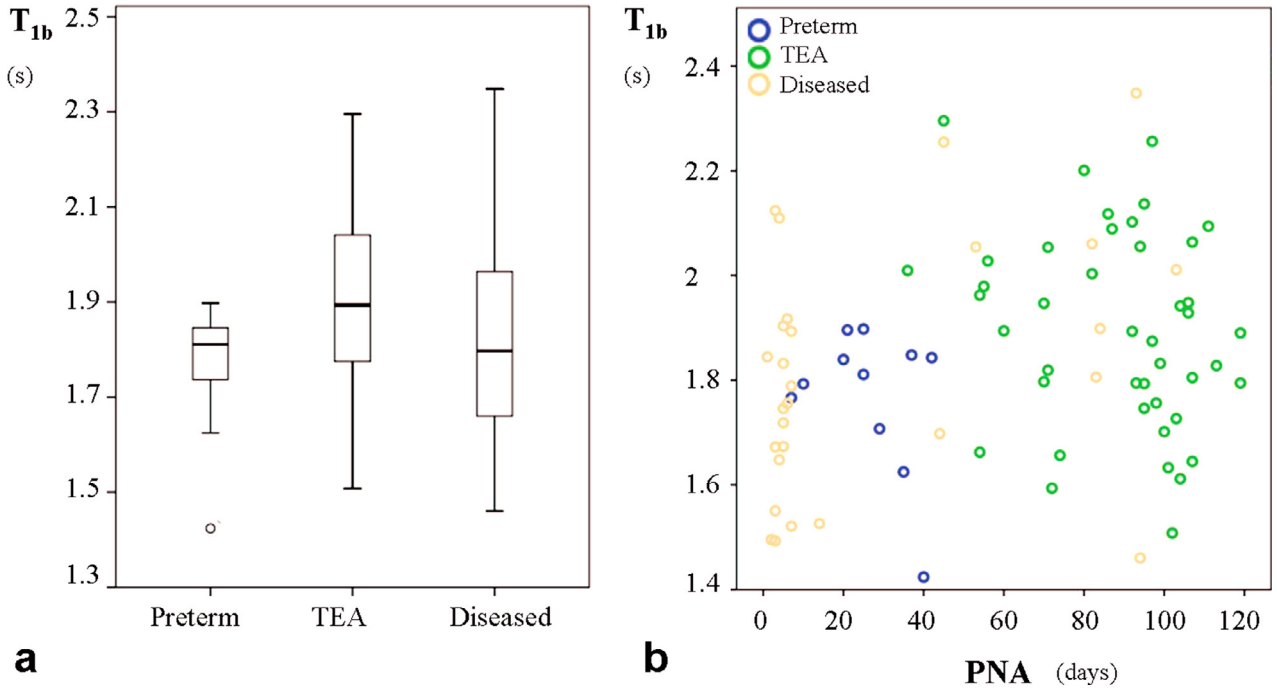

Fig. 2. a) Median, interquartile range, minimum and maximum T_{1b} values (in seconds) for each category; preterms, preterm born infants imaged at term-equivalent age (TEA), and diseased infants which were the infants with a clinical indication for MR imaging. b) The relation between postnatal age (PNA, in days) and the T_{1b} (in seconds) is shown; each category of infants (preterms, TEA and diseased) is shown in a different colour.

Table 3
Cerebral blood flow values in each category.

Group	*N*	$CBF_{1.6}$ (ml/100 g/min)	$CBF_{1.85}$ (ml/100 g/min)	CBF_{cor} (ml/100 g/min)	NPD ($CBF_{cor-1.6}$)	NPD ($CBF_{cor-1.85}$)
Preterm	3 M–6 F	8.5 (6.1)	7.4 (5.3)	8.1 (6.2)	−7 (8.6)%	6.4 (9.9)%
TEA	18 M–23 F	16.6 (7)	14.5 (6.1)	14.4 (6.1)	−13.3 (7.7)%	−0.8 (8.8)%
Diseased	13 M–13 F	21.5 (14.7)	18.8 (12.9)	19.7 (14.5)	−8.6 (10.5)%	4.6 (12)%

In this table mean whole brain perfusion values obtained when quantifying the ASL images with a T_{1b} of 1.6 s ($CBF_{1.6}$), with a T_{1b} of 1.85 s ($CBF_{1.85}$), and with the corrected T_{1b} (CBF_{cor}) are shown for each category; preterm. TEA: preterm born infants with MR imaging at term-equivalent age, diseased: infants with a clinical indication for MR imaging. The number of subjects per category is shown in the column with the heading 'N' with M as the number of male subjects and F as the number of female subjects. The mean (standard deviation) normalized perfusion difference when going from $CBF_{1.6}$ to CBF_{cor} ($CBF_{cor-1.6}$) is shown and the mean (standard deviation) normalized perfusion difference when going from $CBF_{1.85}$ to CBF_{cor} ($CBF_{cor-1.85}$) is shown. The normalized perfusion difference, when going from $CBF_{1.6}$ to CBF_{cor}, was significantly different in preterm than in the TEA ($p < 0.05$).

it can be inferred that the normalized perfusion difference increases with up to 5–10% at low and high Hct values when λ is corrected for haematocrit. There is limited effect of λ on the normalized perfusion difference at haematocrit levels around 0.4–0.45. In other words, by keeping the λ constant has a small compensatory effect on the CBF error.

4. Discussion

We evaluated the T_1 of blood in neonates and found a mean T_{1b} of 1.85 s which is higher than the commonly assumed ≤1.6 s. As expected, a wide variability in the T_{1b}, from 1.4 s to 2.3 s, was observed. So far the T_{1b} was only evaluated in 18 neonates where a similar wide variability was demonstrated (Varela et al., 2011). What our study adds to the previous one is the evaluation of the T_{1b} in categories of neonates. We found that the T_{1b} in preterm born infants was significantly different from the T_{1b} in preterm born infants imaged at term-equivalent age. This corresponded to the differences that we found in haematocrit, preterms had a haematocrit of 0.40 while the preterm born infants at term-equivalent age had a haematocrit of 0.34. Similar results were found in the infants with longitudinal data. Although the decline in haematocrit after birth may support a postnatal age-dependent T_{1b}, it is important to realize that the decline

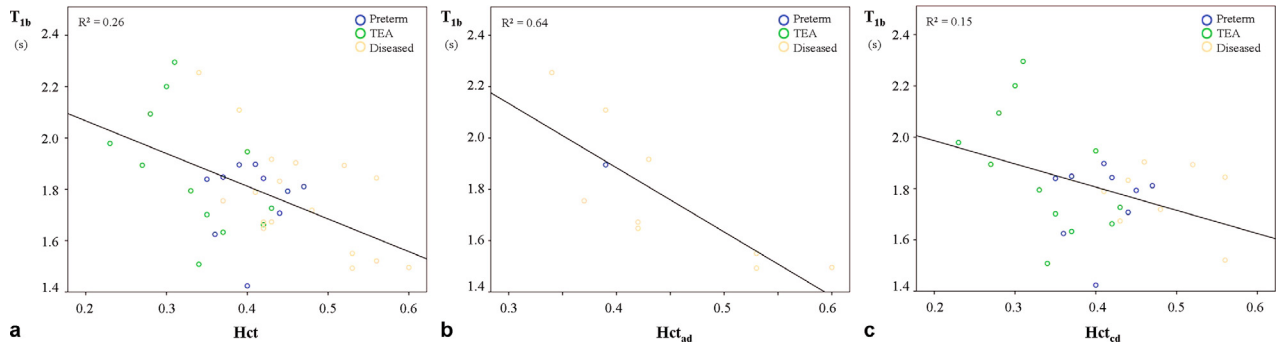

Fig. 3. a) A scatter plot demonstrating the relation between haematocrit (Hct) and MRI-derived T_{1b} (in seconds). b) A scatter plot demonstrating the relation between arterial-drawn haematocrit (Hct_{ad}) and MRI_derived T_{1b} (in seconds). c) A scatter plot demonstrating the relation between capillary-drawn haematocrit (Hct_{cd}) and MRI-derived T_{1b} (in seconds).

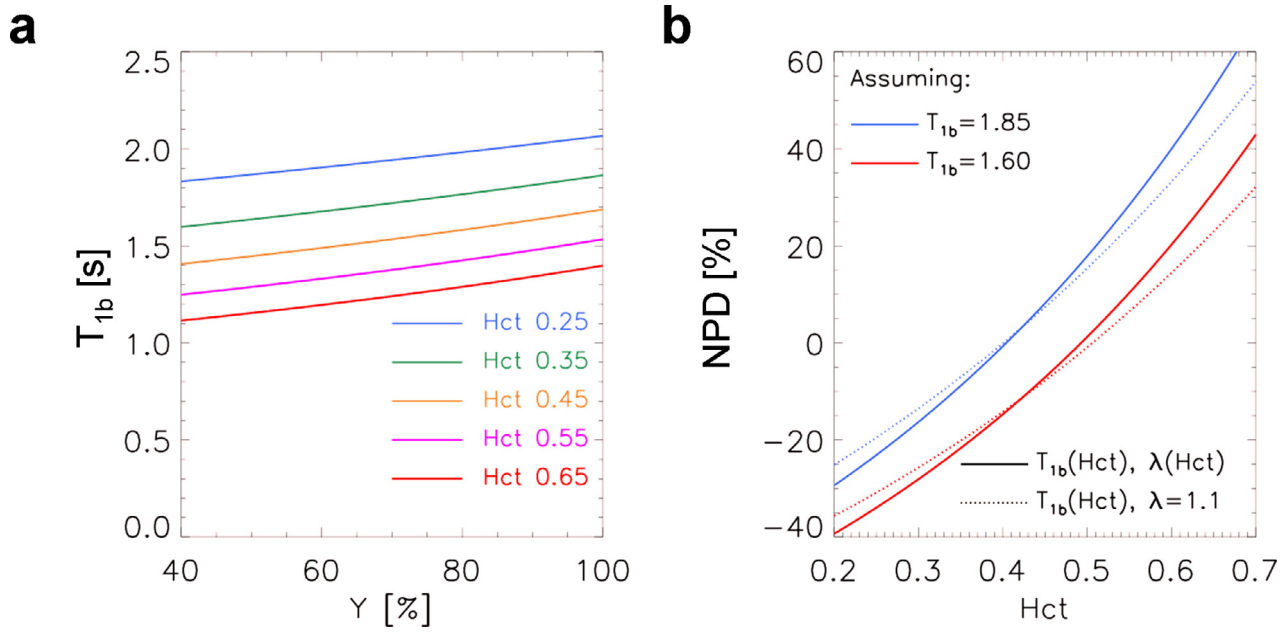

Fig. 4. a) Dependence of the T_{1b} on haematocrit (Hct) and oxygenation (Y). b) Simulation demonstrating the normalized perfusion difference introduced by the influence of haematocrit (Hct) on the T_{1b}, with (full line) and without (dotted line) taking the influence of haematocrit on the brain–blood partition coefficient (λ) into account.

in haematocrit in term born neonates after birth has a shorter timespan compared to the decline in preterms, haematocrit levels restore 4–6 weeks after birth in term neonates (Palis and Segel, 1998). In addition, even within the preterms and the TEA infants the T_{1b} range was wide and overlapping, and a plot demonstrating the relation between the T_{1b} and postnatal age showed a wide variability (Fig. 2b).

The T_{1b} is an important parameter in a range of imaging modalities. Because ASL MR imaging is part of our imaging protocol we used it to demonstrate the importance of estimating the T_{1b} in neonates as it is a parameter needed for quantification. The mean normalized perfusion difference when quantifying CBF with a T_{1b} of 1.6 s as opposed to the corrected T_{1b} value was −11%. Furthermore, we demonstrated that the maturational increase in perfusion is overestimated when quantifying CBF with a fixed T_{1b} of 1.6 s. A similar overestimation of the maturational increase in perfusion was found in 4 infants with serial MR imaging at preterm and term-equivalent age. In this study we choose a T_{1b} of 1.6 s as the reference value as this was used in a recent neonatal ASL study (Massaro et al., 2013). However, values of 1.5 s have also been reported (Miranda et al., 2006; Wintermark et al., 2011) and would make the normalized perfusion difference even larger. Our findings clearly demonstrate that the T_{1b} should be corrected when performing T_{1b}-dependent MRI studies in neonates and that it is in particular important when the studies are of longitudinal origin. Although we demonstrated that a more appropriate neonatal T_{1b} probably resides around 1.85 s, adopting this value in ASL studies would only shift the global mean of neonatal CBF but it would not account for the variations due to e.g. postnatal age. Applying the group mean T_{1b} of 1.85 s obtained in this study instead of an individual-obtained T_{1b} eliminated the average normalized perfusion difference while the range still remained wide (−16.8% to +29.9%). As is shown in Fig. 2, there is a large spread of T_{1b} (and Hct) within each group and even when applying an individual-obtained T_{1b} the spread in the CBF estimates remains in the same range within the groups (Table 3). Important for the reader to note is that not only the T_{1b} but also the brain–blood partition coefficient (λ) is dependent on haematocrit (Herscovitch and Raichle, 1985). This was not taken into account when calculating the normalized perfusion difference. However, λ is linearly related to cerebral blood flow whereas T_{1b} has an exponential relation and thus the effect of λ on the normalized perfusion difference is less. This was demonstrated by a simulation which showed that the effect of haematocrit on λ may increase the normalized perfusion difference with another 5%.

Blood T_1 sequences and their postprocessing tools are not readily available on most MR platforms. Therefore, a good alternative would

be to estimate T_{1b} from haematocrit which in most cases is available around the time of MR imaging. In order to test the reliability of the earlier established relationships between the T_{1b} and haematocrit when using a point-of-care device to measure haematocrit, we analysed the relation between haematocrit, determined by means of a conductivity-based point-of-care device, and the T_{1b}. Contrary to the earlier studies in which a sedimentation or spinning technique was used (Lu et al., 2004; Varela et al., 2011), we found only a moderate relation ($R^2 = 0.249$, $p < 0.01$, $R_{1b} = 0.38 \times Hct + 0.40$). This relation did fall within the 95%-confidence interval of the relation previously found by Varela et al.; $R_{1b} = 0.5 \times Hct + 0.37$ (Varela et al., 2011). We know that the haematocrit is by itself susceptible to noise as posture (Jacob et al., 2005), punctuate location and sample (arterial-drawn, capillary-drawn or venous-drawn sample) (Kayiran et al., 2003; Ozbek et al., 2000) can influence its results. Therefore, we subdivided the samples into arterial-drawn and capillary-drawn and interestingly enough we discovered a strong relation with arterial-drawn haematocrit ($R^2 = 0.711$, $p < 0.01$) but a weak and nonsignificant relation between capillary-drawn haematocrit and T_{1b}. There could be several reasons for the lack of correlation in the capillary-drawn samples. First, the infants in whom the capillary measurements were performed might have had less reliable T_{1b} measurements, in fact there were more preterms and TEA present in the capillary-drawn group than in the group with arterial samples and we found a broader 95% confidence interval of the T_{1b} fitting in the preterms compared to the other categories. Another plausible cause could be that the infants in whom the capillary measurements were performed might have had a larger spread of the venous oxygenation. In fact, more preterms were ventilated and we found the relation between R_1 of blood and haematocrit to be nonsignificant in the ventilated infants suggesting an influence of oxygenation on the T_{1b}–haematocrit relation. The T_{1b} is known to be related to both haematocrit and oxygenation (Grgac et al., 2012) and therefore to give some insight into the potential errors due to the oxygenation status on the T_{1b} estimate, simulations are shown in Fig. 3a. This figure demonstrates that a realistic fluctuation of ~20% in venous oxygenation may give rise to a 100 ms difference in T_{1b}. This would translate into an error of ± 0.1 in the haematocrit, at most. While there might be errors in the T_{1b} estimate related to the population bias of the neonates with capillary-drawn Hct, we still speculate that the main reason for this weak Hct–T_{1b} relationship is due to uncertainties in the actual measured capillary haematocrit. The arterial-drawn T_{1b}–Hct relationship on the other hand showed a strong correlation ($R^2 = 0.711$, $p < 0.01$). This relation ($R_{1b} = 0.80 \times Hct_{ad} + 0.22$) was within the error margins of the relationship found by Lu et al. in venous blood ($R_{1b} = 0.83 \times Hct + 0.28$) (Lu et al., 2004). The relationship deviates somehow from the one reported by Varela et al. (2011), although our 95% confidence interval also encompasses their solution. Again, a plausible explanation could be attributed to differences in oxygenation levels in the sagittal sinus. While Lu et al. maintained a constant oxygen saturation (69%) in an in-vitro experiment on bovine blood (Lu et al., 2004), then neither the current study nor the one of Varela et al. (2011) controlled for venous oxygenation. Nevertheless, our results do suggest that the neonatal T_{1b} can be derived from arterial-drawn haematocrit measured by means of a point-of-care device. Despite this, one should always be careful that the haematocrit measurements are not influenced by hypoproteinaemia (Abbott Point of Care Inc., 2013), hyperlipidaemia (Proytcheva, 2009) or drugs (Young et al., 1975). As we did not have information about the drugs administered to the neonates we could not investigate the impact of drugs on haematocrit and consequently the haematocrit–T_{1b} relation.

There are some limitations to this study. First, as mentioned above, we did not take into account the effect of venous oxygenation on our T_{1b} values although simulations demonstrate that venous oxygenation can have an effect on the T_{1b}. This may explain why the relation between haematocrit and the T_{1b} was not as strong as previously published relations. In this regard we should mention that the T_{1b} expected for ASL CBF quantification is the arterial T_{1b} while we measured the venous. It is hard to do a correction for this without knowledge of the actual venous blood oxygenation and the haematocrit, although at 3 T and at typical venous oxygenation levels the T_{1b} is approximately 100 ms shorter than the arterial T_{1b} (Lu et al., 2004; Shimada et al., 2012) which is also illustrated in Fig. 3a. The reasons for not measuring arterial blood directly are manifold. In the neonates the blood vessels are very small and even within the sagittal sinus, targeted in this study, only 5 voxels could be used on average. The feeding arterial vessels are even smaller making partial volume and small scale motion a problem. In addition the higher blood velocities and highly pulsatile flow complicate accurate acquisition and subsequent T_1 quantification. While not a problem in neonates, then older children and adults extend outside the transmit coil, contaminating the inversion recovering arterial blood with fresh fully relaxed blood.

In addition, we investigated the influence of haematocrit on the T_{1b} and how it influenced the brain–blood partition coefficient (λ) which is also used for quantification. We demonstrated that the normalized perfusion difference introduced by the effect of haematocrit on λ is minor compared to the normalized perfusion difference caused by the T_{1b} assumption. It should be mentioned that λ does not only depend on the neonates' haematocrit but also on the brains' water content which is known to decrease after birth (Dobbing et al., 1973; Kreis et al., 1993) and this was not taken into account in our simulations. However, there are some other factors which potentially could have affected the CBF differences in between groups and which may affect the CBF during longitudinal follow-up. The most important one would be the label bolus arrival time which potentially could be dependent on postnatal age. In this study we used a Q_2TIPS scheme which ensures a well-defined bolus length and thereby makes the CBF estimate less sensitive to differences in arrival time (Luh et al., 1999). Nevertheless, little is known about the validity of the assumptions made during quantification in the neonates, the main reason being the fact that typically very little time is allocated to experimental scans before sedation wears out. Future studies should investigate if for instance the generated bolus fulfils the requirement of being longer than TI_1, and how big an error is introduced by assuming no exchange and ignoring the arterial transit time ($q = 1$ in Eq. (2) of Luh et al. 1999). A general problem with ASL in neonates is the poor signal to noise in the perfusion maps and this is regardless of the generally longer T_1 of blood observed in neonates compared to adults. The longer T_1 of blood would result in a longer lasting label bolus, however, due to the intrinsic low perfusion in neonates and the fact that motion can be a problem, the signal to noise remains low. Hardware improvements and optimization of e.g. pseudocontinuous ASL for the neonates may improve the situation, however, good strategies for efficient dealing with motion may be even more beneficial in this patient population. For instance, the potential benefits of high signal-to-noise 3D readout strategies with subsequent image registration and prospective motion correction schemes should be investigated in the future.

Lastly, as our scans were performed at the end of a clinical imaging protocol, when sedation started to wear of, we experienced motion issues. This was reflected in an unsuccessful fitting of the T_{1b} in 32% of the neonates primarily caused due to excessive image noise or patient motion resulting in a non-converging fit. In other instances it was impossible to detect a region of interest in the sagittal sinus region.

In conclusion, we confirmed the wide variability of T_{1b} in neonates and demonstrated differences between preterms and preterms at term-equivalent age related to changes in haematocrit. This study suggests that the T_{1b} should be corrected when performing blood-T_1 dependent MRI studies in neonates such as ASL perfusion imaging. The relation between arterial-drawn haematocrit, measured with a point-of-care device, and the T_{1b} was similar to the earlier described

one which relied on spinning or sedimentation techniques to determine the haematocrit. Therefore, the T_{1b} derived from arterial-drawn haematocrit as measured by a point-of-care device can be a good approach to estimate the T_{1b} in neonates until established T_{1b}-sequences are standard on the scanners. However we also showed that capillary-drawn Hct values have limited value and should be avoided when inferring blood T_1 from haematocrit. In neonates without an arterial-drawn blood sample one can always choose to use a more appropriate neonatal T_{1b} value to minimize the normalized perfusion difference. For instance 1.85 s which was the mean T_{1b} value found in our population or a preterm or term-equivalent values as reported in Table 3, if applicable.

Grant support

This research is supported by the Dutch Technology Foundation STW, Applied Science Division of NWO, the Technology Program of the Ministry of Economic Affairs and the ZonMW Electromagnetic Fields and Health Program.

References

Abbott Point of Care Inc., 25-01-2014, Hematocrit/Hct and calculated hemoglobin/Hb. ⟨5:underline ⟩http://www.abbottpointofcare.com⟨/5:underline⟩

Buxton, R.B., 2005. Quantifying CBF with arterial spin labeling. Journal of Magnetic Resonance imaging: JMRI 22, 723–6. http://dx.doi.org/10.1002/jmri.20462, 16261574.

Chanarin, I., 1984. Blood and Its Disease. New York: Churchill Livingstone.

Christensen, R.D, 2000. Hematologic Problems of the Neonate. Philadelphia. W. B. Saunders, pp. 117–36.

Dobbing, J., Sands, J., 1973. Quantitative growth and development of human brain. Archives of Disease in Childhood 48, 757–67. http://dx.doi.org/10.1136/adc.48.10.757, 4796010.

Edelman, R.R., Chien, D., Kim, D., 1991. Fast selective black blood MR imaging. Radiology 181, 655–60, 1947077.

Efron, B, 1979. Bootstrap methods: another look at the jackknife. The Annals of Statistics 7, 1–26. http://dx.doi.org/10.1214/aos/1176344552.

Ehrnebo, M., Agurell, S., Jalling, B., Boréus, L.O., 1971. Age differences in drug binding by plasma proteins: studies on human foetuses, neonates and adults. European Journal of Clinical Pharmacology 3, 189–93. http://dx.doi.org/10.1007/BF00565004, 5151301.

Farahani, K., Saxton, R.E., Yoon, H.C., De, Salles A.A., Black, K.L., Lufkin, R.B., 1999. MRI of thermally denatured blood: methemoglobin formation and relaxation effects. Magnetic Resonance imaging 17, 1489–94. http://dx.doi.org/10.1016/S0730-725X(99)00094-6, 10609997.

Geaghan, S. (2005), Normal Blood Values: Selected Reference Values for Neonatal, Pediatric and Adult Populations. Hematology, Basic Principles and Practice. Elsevier — Churchill Livingstoner, Philadelphia

Gevers, S., van Osch, M.J., Bokkers, R.P., Kies, D.A., Teeuwisse, W.M., Majoie, C.B. et al, 2011. Intra- and multicenter reproducibility of pulsed, continuous and pseudo-continuous arterial spin labeling methods for measuring cerebral perfusion. Journal of Cerebral Blood Flow and Metabolism: Official Journal of the International Society of Cerebral Blood Flow and Metabolism 31, 1706–15. http://dx.doi.org/10.1038/jcbfm.2011.10, 21304555.

Golay, X., Petersen, E.T., Hui, F., 2005. Pulsed star labeling of arterial regions (PULSAR): a robust regional perfusion technique for high field imaging. Magnetic Resonance in Medicine: Official Journal of the Society of Magnetic Resonance in Medicine / Society of Magnetic Resonance in Medicine 53, 15–21. http://dx.doi.org/10.1002/mrm.20338, 15690497.

Grgac, K., van Zijl, P.C., Qin, Q., 2012. Hematocrit and oxygenation dependence of blood (1) H(2)O T(1) at 7 tesla. Magnetic Resonance in Medicine. http://dx.doi.org/10.1002/mrm.24547.

Herscovitch, P., Raichle, M.E., 1985. What is the correct value for the brain–blood partition coefficient for water? Journal of Cerebral Blood Flow and Metabolism: Official Journal of the International Society of Cerebral Blood Flow and Metabolism 5, 65–9. http://dx.doi.org/10.1038/jcbfm.1985.9, 3871783.

Jacob, G., Raj, S.R., Ketch, T., Pavlin, B., Biaggioni, I., Ertl, A.C. et al, 2005. Postural pseudoanemia: posture-dependent change in hematocrit. Mayo Clinic Proceedings 80, 611–14. http://dx.doi.org/10.4065/80.5.611, 15887428.

Jopling, J., Henry, E., Wiedmeier, S.E., Christensen, R.D., 2009. Reference ranges for hematocrit and blood hemoglobin concentration during the neonatal period: data from a multihospital health care system. Pediatrics 123, e333–e337, 19171584.

Kayiran, S.M., Ozbek, N., Turan, M., Gürakan, B., 2003. Significant differences between capillary and venous complete blood counts in the neonatal period. Clinical and Laboratory Haematology 25, 9–16. http://dx.doi.org/10.1046/j.1365-2257.2003.00484.x, 12542436.

Kreis, R., Ernst, T., Ross, B.D., 1993. Development of the human brain: in vivo quantification of metabolite and water content with proton magnetic resonance spectroscopy. Magnetic Resonance in Medicine: Official Journal of the Society of Magnetic Resonance in Medicine / Society of Magnetic Resonance in Medicine 30, 424–37. http://dx.doi.org/10.1002/mrm.1910300405, 8255190.

Lu, H., Clingman, C., Golay, X., van Zijl, P.C., 2004. Determining the longitudinal relaxation time (T1) of blood at 3.0 tesla. Magnetic Resonance in Medicine: Official Journal of the Society of Magnetic Resonance in Medicine / Society of Magnetic Resonance in Medicine 52, 679–82. http://dx.doi.org/10.1002/mrm.20178, 15334591.

Lu, H., Golay, X., Pekar, J.J., Van Zijl, P.C., 2003. Functional magnetic resonance imaging based on changes in vascular space occupancy. Magnetic Resonance in Medicine: Official Journal of the Society of Magnetic Resonance in Medicine / Society of Magnetic Resonance in Medicine 50, 263–74. http://dx.doi.org/10.1002/mrm.10519, 12876702.

Luh, W.M., Wong, E.C., Bandettini, P.A., Hyde, J.S., 1999. Quips II with thin-slice TI1 periodic saturation: a method for improving accuracy of quantitative perfusion imaging using pulsed arterial spin labeling. Magnetic Resonance in Medicine: Official Journal of the Society of Magnetic Resonance in Medicine / Society of Magnetic Resonance in Medicine **41** (, 1246–54. http://dx.doi.org/10.1002/(SICI)1522-2594(199906)41:6<1246::AID-MRM22>3.0.CO;2-N, 10371458.

Massaro, A.N., Bouyssi-Kobar, M., Chang, T., Vezina, L.G., du Plessis, A.J., Limperopoulos, C., 2013. Brain perfusion in encephalopathic newborns after therapeutic hypothermia. AJNR. American Journal of Neuroradiology 34, 1649–55. http://dx.doi.org/10.3174/ajnr.A3422, 23493898.

Miranda, M.J., Olofsson, K., Sidaros, K., 2006. Noninvasive measurements of regional cerebral perfusion in preterm and term neonates by magnetic resonance arterial spin labeling. Pediatric Research 60, 359–63. http://dx.doi.org/10.1203/01.pdr.0000232785.00965.b3, 16857776.

Oguz, K.K., Golay, X., Pizzini, F.B., Freer, C.A., Winrow, N., Ichord, R. et al, 2003. Sickle cell disease: continuous arterial spin-labeling perfusion MR imaging in children. Radiology 227, 567–74. http://dx.doi.org/10.1148/radiol.2272020903, 12663827.

Ozbek, N., Gürakan, B., Kayiran, S.M., 2000. Complete blood cell counts in capillary and venous blood of healthy term newborns. Acta Haematologica 103, 226–8. http://dx.doi.org/10.1159/000041056, 11014900.

Palis, J., Segel, G.B., 1998. Developmental biology of erythropoiesis. Blood Reviews 12, 106–14. http://dx.doi.org/10.1016/S0268-960X(98)90022-4, 9661799.

Papa, F., Rongioletti, M., Ventura, M.D., Di, Turi F., Cortesi, M., Pasqualetti, P. et al, 2011. Blood cell counting in neonates: a comparison between a low volume micromethod and the standard laboratory method. Blood Transfusion = Trasfusione Del Sangue 9, 400–6, 21839016.

Proytcheva, M.A, 2009. Issues in neonatal cellular analysis. American Journal of Clinical Pathology 131, 560–73. http://dx.doi.org/10.1309/AJCPTHBJ4I4YGZQC, 19289592.

Qin, Q., Strouse, J.J., van Zijl, P.C., 2011. Fast measurement of blood T1 in the human jugular vein at 3 tesla. Magnetic Resonance in Medicine: Official Journal of the Society of Magnetic Resonance in Medicine / Society of Magnetic Resonance in Medicine 65, 1297–304. http://dx.doi.org/10.1002/mrm.22723, 21500258.

Salsbury, D.C, 2001. Anemia of prematurity. Neonatal Network: NN 20, 13–20. http://dx.doi.org/10.1891/0730-0832.20.4.1310.1891/0730-0832.20.5, 12144218.

Shimada, K., Nagasaka, T., Shidahara, M., Machida, Y., Tamura, H., 2012. In vivo measurement of longitudinal relaxation time of human blood by inversion-recovery fast gradient-echo MR imaging at 3 T. Magn. Resonance Medical Science 11, 265–71. http://dx.doi.org/10.2463/mrms.11.265.

Silvennoinen, M.J., Kettunen, M.I., Kauppinen, R.A., 2003. Effects of hematocrit and oxygen saturation level on blood spin-lattice relaxation. Magnetic Resonance in Medicine: Official Journal of the Society of Magnetic Resonance in Medicine / Society of Magnetic Resonance in Medicine 49, 568–71. http://dx.doi.org/10.1002/mrm.10370, 12594761.

Varela, M., Hajnal, J.V., Petersen, E.T., Golay, X., Merchant, N., Larkman, D.J., 2011. A method for rapid in vivo measurement of blood T1. N.M.R. in Biomedicine 24, 80–8. http://dx.doi.org/10.1002/nbm.1559.

Williams, D.S., Detre, J.A., Leigh, J.S., Koretsky, A.P., 1992. Magnetic resonance imaging of perfusion using spin inversion of arterial water. Proceedings of the National Academy of Sciences of the United States of America 89, 212–16. http://dx.doi.org/10.1073/pnas.89.1.212, 1729691.

Wintermark, P., Hansen, A., Gregas, M.C., Soul, J., Labrecque, M., Robertson, R.L. et al, 2011. Brain perfusion in asphyxiated newborns treated with therapeutic hypothermia. AJNR. American Journal of Neuroradiology 32, 2023–9. http://dx.doi.org/10.3174/ajnr.A2708, 21979494.

Wu, W.C., Jain, V., Li, C., Giannetta, M., Hurt, H., Wehrli, F.W. et al, 2010. In vivo venous blood T1 measurement using inversion recovery true-FISP in children and adults. Magnetic Resonance in Medicine: Official Journal of the Society of Magnetic Resonance in Medicine / Society of Magnetic Resonance in Medicine 64, 1140–7. http://dx.doi.org/10.1002/mrm.22484, 20564586.

Young, D.S., Pestaner, L.C., Gibberman, V., 1975. Effects of drugs on clinical laboratory tests. Clinical Chemistry 21, 1D–432D, 1091375.